SUPPORTING INFORMATION:

Controlling Differentiation of Adipose-Derived Stem Cells Using Combinatorial Graphene Hybrid-Pattern Arrays

Tae-Hyung Kim[a,d†], Shreyas Shah[a†], Letao Yang[a], Perry T. Yin[b], Khaled A. Hossain[e], Brian Conley[c], Jeong-Woo Choi[d,e*] and Ki-Bum Lee[a,b*]

[a]*Department of Chemistry and Chemical Biology, Rutgers, The State University of New Jersey*

610 Taylor Road, Piscataway, NJ 08854, USA

[b]*Department of Biomedical Engineering, Rutgers, The State University of New Jersey*

610 Taylor Road, Piscataway, NJ 08854, USA

[c]*Department of Cell Biology and Neuroscience, Rutgers, The State University of New Jersey*

610 Taylor Road, Piscataway, NJ 08854, USA

[d]*Department of Chemical & Biomolecular Engineering, Sogang University*

35 Baekbeom-ro, Mapo-gu, Seoul 121-742, Republic of Korea

[e]*Interdisciplinary Program of Integrated Biotechnology, Sogang University,*

#1 Shinsu-Dong, Mapo-Gu, Seoul 121-742, Republic of Korea

***Correspondence:**

Prof. Jeong-Woo Choi
Department of Chemical & Biomolecular Engineering
Sogang University, Seoul, South Korea
Tel. +82-2-705-8480; Fax: +82-2-3273-0331.
E-mail: jwchoi@sogang.ac.kr

Prof. Ki-Bum Lee

Department of Chemistry and Chemical Biology, Rutgers, The State University of New Jersey
610 Taylor Road, Piscataway, NJ 08854, USA
Tel. +1-732-445-2081; Fax: +1-732-445-5312
E-mail: kblee@chem.rutgers.edu

http://kblee.rutgers.edu/

A. EXPERIMENTAL SECTION

Materials and cells (hADMSCs)

Material characterizations

Generation of protein patterns

B. SUPPLEMENTARY FIGURES

Supplementary Fig. 1	Characterization of NGO & NGO combinatorial patterns
Supplementary Fig. 2	Helium ion microscopic images of small-sized NGO grid patterns
Supplementary Fig. 3	Confocal Raman mapping of NGO line patterns on gold substrate
Supplementary Fig. 4	AFM analysis of NGO square pattern on gold substrate
Supplementary Fig. 5	NGO square patterns on tissue culture plate analyzed by confocal Raman spectroscopy
Supplementary Fig. 6	High stability of NGO pattern on gold substrate confirmed by Raman spectroscopy after ultrasonic cleaning
Supplementary Fig. 7	Actin-stained images of hADMSCs on glass, gold, NGO-coated gold, NGO line and NGO grid patterns
Supplementary Fig. 8	Comparison of hADMSC osteogenesis on different substrates.
Supplementary Fig. 9	Size-dependent effect of NGO line patterns on osteogenesis of hADMSCs
Supplementary Fig. 10	Neuronal differentiation of hADMSCs on laminin (LN)-coated substrates.

A. EXPERIMENTAL SECTION

Materials and Cells (hADMSCs)

Gold substrates were prepared by depositing chromium (99.999%, International Advanced Materials, USA) and gold (99.999%, International Advanced Materials, USA) on the cover glass with thickness of 2nm and 50nm, respectively, using E-beam evaporator (Applied Materials, USA). PDMS (Sylgard 184) were purchased from Dow Corning. (Heptadecafluoro-1,1,2,2-tetrahydrocecyl)trichlorosilane were obtained from Gelest Inc. Human/Rat Osteocalcin MAb (Clone 190125, Mouse IgG1) was purchased from R&D systems. Neuronal class III β-Tubulin (TUJ1) monoclonal antibody (MMS-435P, Mouse IgG2a) was obtained from BioLegend. Dexamethasone, ascorbic acid, β-Glycerophosphate, Poly-L-lysine (PLL) and retinoic acid (RA) were obtained from Sigma-Aldrich, USA. Hank's balanced salt solution (HBSS), DMEM, DPBS, TrypLE, Alexa Fluor® 546 Phalloidin, Alexa Fluor® 546 Goat Anti-Mouse IgG and Hoechst were purchased from Life Technologies. Fibronectin and laminin were obtained from Millipore, USA. Human recombinant brain derived neurotrophic factor (BDNF), basic fibroblast growth factor (bFGF) and epidermal growth factor (EGF) were obtained from Peprotech. EG4-(CH2)11-SH were synthesized by our group as previously reported. Human adipose-derived mesenchymal stem cells (hADMSCs) derived from 29- and 63-year-old woman patient (p=0) and 0.5% FBS ACS medium were kindly donated by American CryoStem, (Edison, New Jersey, USA). Other chemicals used in this study were obtained commercially and were of reagent grade.

Material characterizations

Topcon 002B TEM was used (200 kV) to obtain a transmission electron micrographs of NGO. To prepare the sample for TEM imaging, 0.1 mg/ml NGO solution was dropped on standard

TEM grids and subjected to vacuum drying. Zetasizer (ZS Nano, Malvern Instruments) was used to analyze both hydrodynamic size and zeta potential of NGO (1.0 mg/ml at 25 ºC with a detection angle of 90º). The size and zeta potential values of NGO were averaged from 11 replicates. UV-Vis spectrum of NGO was measured using Agilent Cary 60 UV-Vis spectrometer. To confirm the stability of NGO pattern on gold substrate, Raman spectra was obtained using Renishaw inVia Raman microscope (1200gr/mm @633nm) by averaging signals which were accumulated for three times. For XPS (X-ray Photoelectron Spectroscopy) analysis, the NGO was spin-coated on the surface of Si substrate and dried under vacuum for overnight. The NGO coated Si substrate was then analyzed by XPS (Thermo Scientific, ESCALAB 250Xi) under a base pressure of 1×10^{-9} Torr. The core level spectra was obtained by an Al-Kα monochromated X-ray source with 0.5 eV total instrumental broadening. Peak fitting was conducted using XPS viewer software.

AFM images and Raman mapping were obtained using NTEGRA spectra (AFM-Raman Spectrometer, NT-MDT, Russia) equipped with a liquid nitrogen-cooled CCD camera and an inverted microscope (Olympus IX71). Semi-contact mode was used to detect the topological characteristics of NGO patterns on gold substrate. The cantilever (NSG01) used in this study had a typical resonant frequency in the range of 115 to 190 kHz and a force constant of 2.5 to 10N/m. In the case of Raman mapping, the area where NGO patterns generated was first visualized by optical microscope (Olympus IX71) and scanned by laser while full Raman spectrum was recorded to generate 2D mapping images. The resolution of the spectrometer in the XY plane was 200 nm and along the Z axis was 500 nm. Raman spectra were recorded using a laser emitting light at a wavelength of 633 nm. The laser was exposed for 5 seconds at each points to achieve Raman mapping images composed of 64 × 64 dots. After the achievement of Raman

mapping data, the focus of laser was moved to NGO patterned or non-patterned area and the detection for Raman was increased to 20s to check the presence of NGO on each area more precisely.

ORION PLUS Helium-Ion Microscope (Carl Zeiss AG, Germany) was used to image different types of NGO patterns on various kinds of substrates including non-conducting materials without metal coating.

Generation of protein patterns

PDMS stamp was coated with 3mM 1-octadecanethiol (1-ODT) solution and stamped on piranha-cleaned gold/glass substrates for 3 minutes. The ODT-patterned gold substrates were then immersed in 2mM SH-C_{11}-EG_4-OH solution and kept for 12 hours for passivation that prevent protein absorption. After 3 times of washing with ethanol, substrates were moved to 24 well tissue culture plate and exposed to the solution containing fibronectin or laminin. The solutions were kept for 4 hours at RT and washed two times with DPBS to remove the excess proteins. The fibronectin- and laminin-patterned substrates were used for the osteogenesis and neurogenesis of hADMSCs, respectively.

B. SUPPLEMENTARY FIGURES

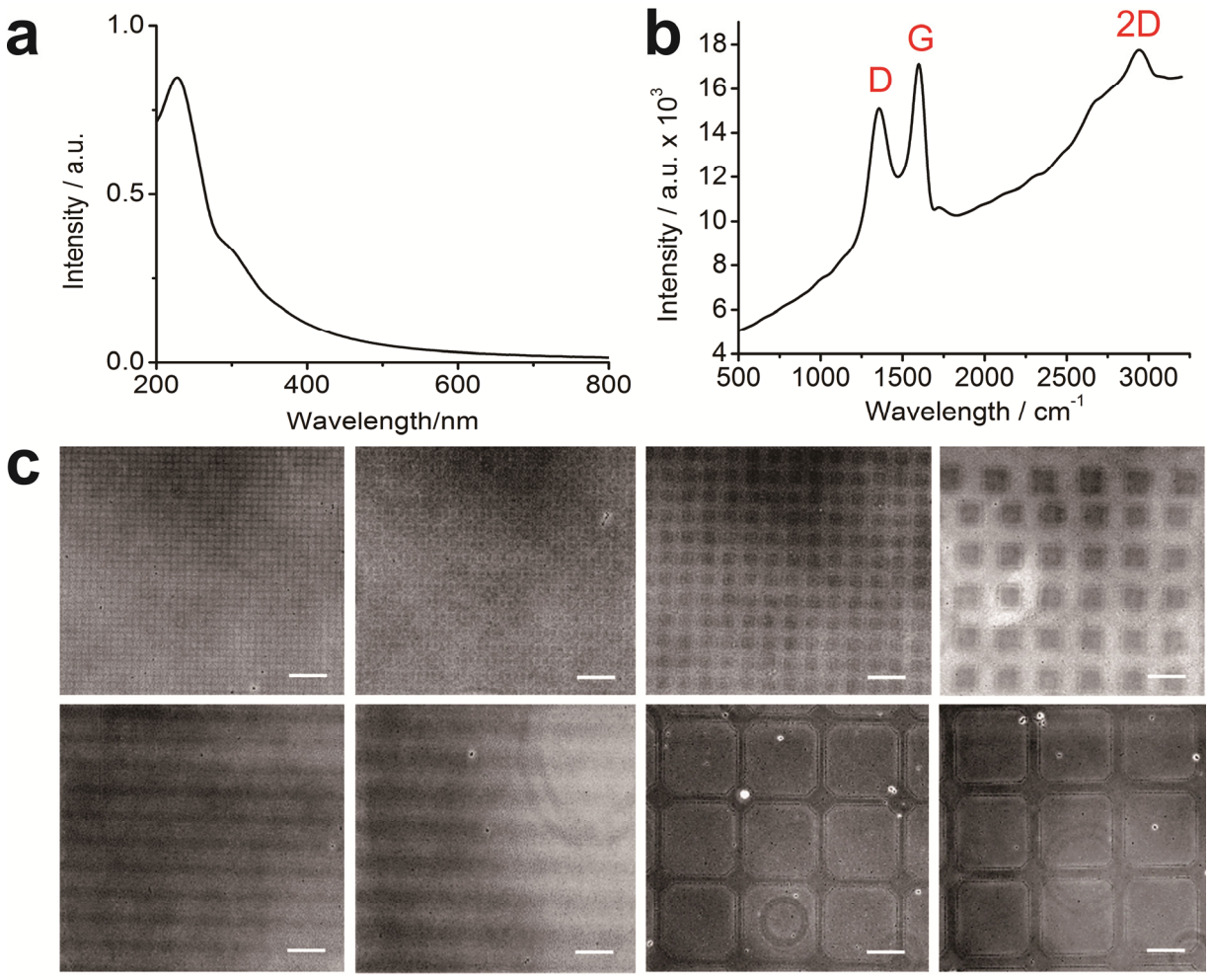

Supplementary Fig. 1 (a) UV/Vis spectra obtained from NGO-containing solution. (b) Raman spectra of NGO patterns on gold-coated glass substrate that shows clear D, G and 2D band. (c) Large-scale image of NGO micropatterns with different size and shape (square, line and grid) imaged by optical microscope. Scale bar = 100μm.

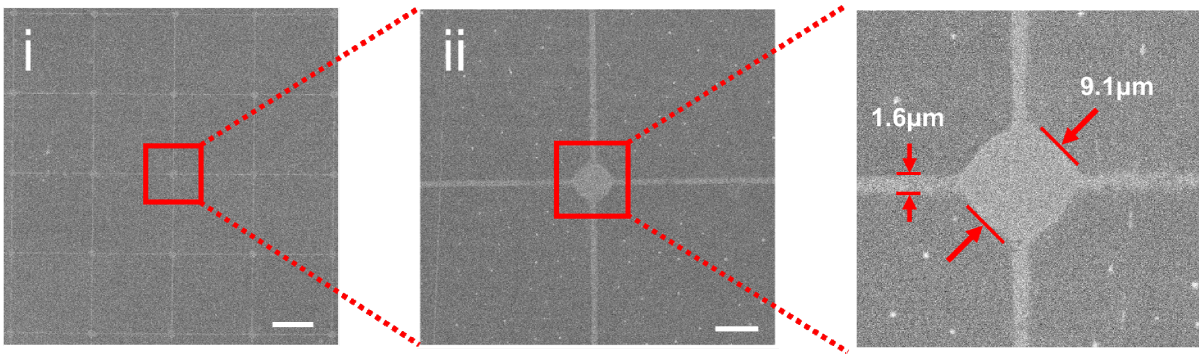

Supplementary Fig. 2 NGO grid pattern generated on the surface of gold. Scale bar = 50μm and 10μm for i) and ii), respectively.

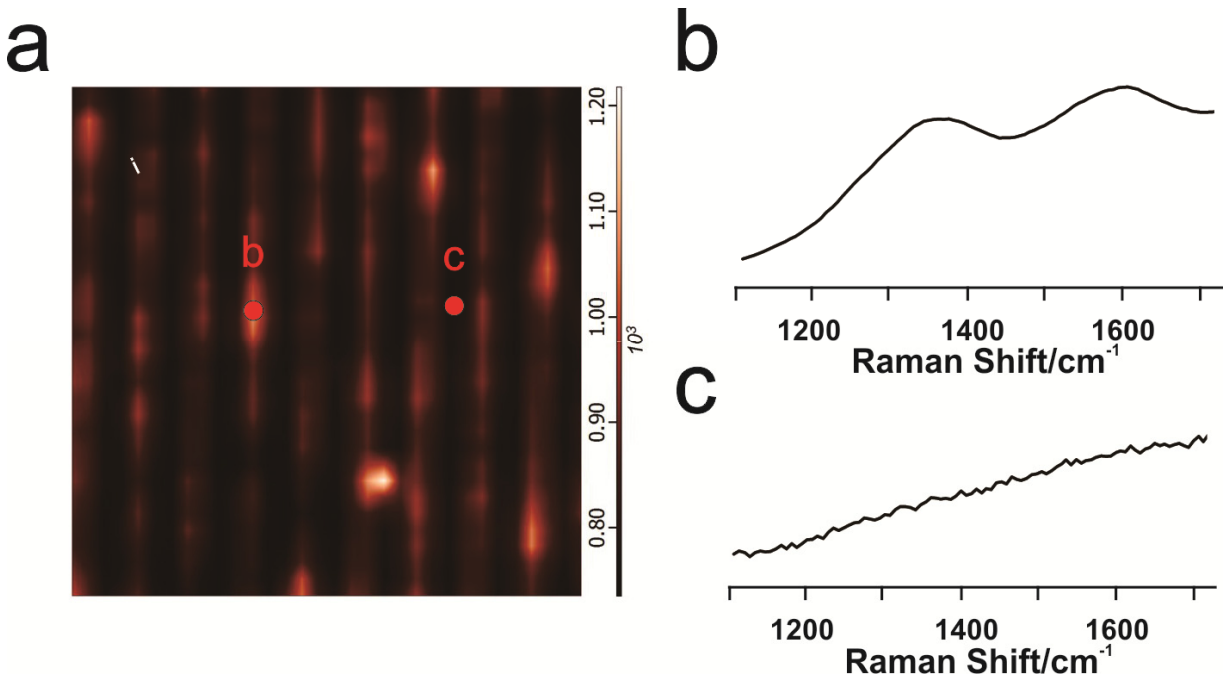

Supplementary Fig. 3 (a) Raman mapping image of NGO line pattern on gold substrate using 'G band (1570cm^{-1})' as an indicator of intensity. (b) and (c) are Raman spectra obtained from spot 'b' and 'c' marked on (a). Exposure time to achieve Raman spectra was 5 seconds and 20 seconds for (a), and (b), (c), respectively.

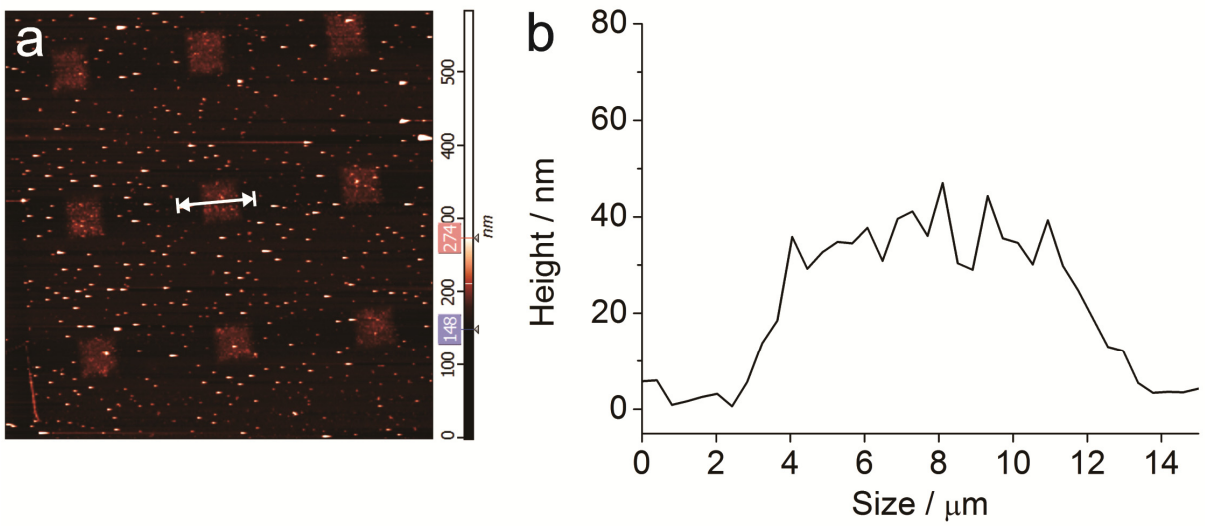

Supplementary Fig. 4 (a) AFM image and (b) height profile of NGO square pattern formed on gold substrate. Size of NGO square pattern imaged by AFM was approximately 10μm.

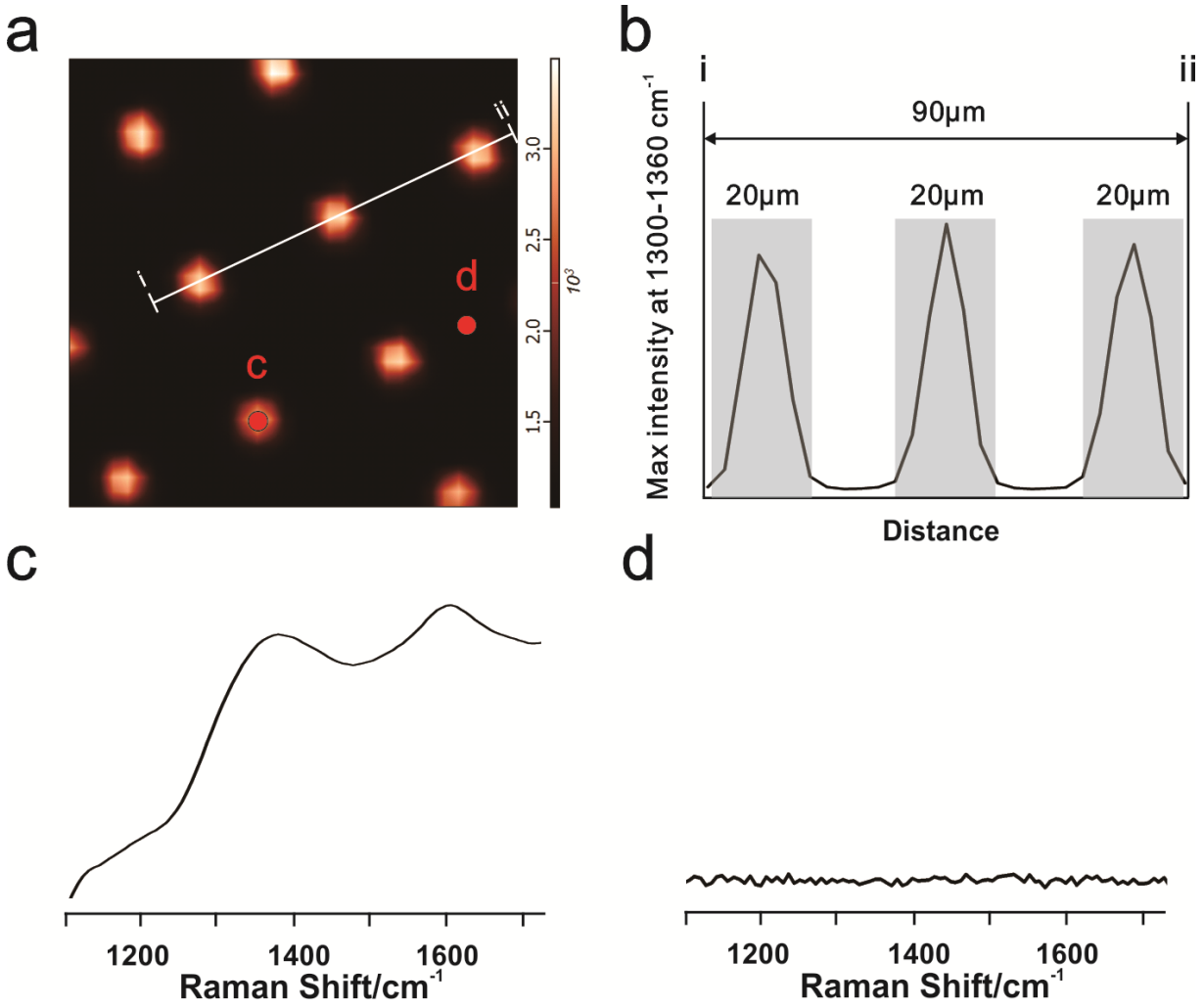

Supplementary Fig. 5 (a) Raman mapping image of NGO square patterns on tissue culture plate (TCP) using 'G band (1570cm^{-1})' as an indicator of intensity. (b) Intensity profile of Raman signals from spot 'i' to spot 'ii' on the Raman mapping image. The regions where Raman intensity increased were marked as grey color that matches with the size of NGO pattern. (c) and (d) are Raman spectra obtained from spot 'c' and 'd' on (a), proving presence and absence of NGO. Exposure time to achieve Raman spectra was 5 seconds and 20 seconds for (a), (b) and (c), (d), respectively.

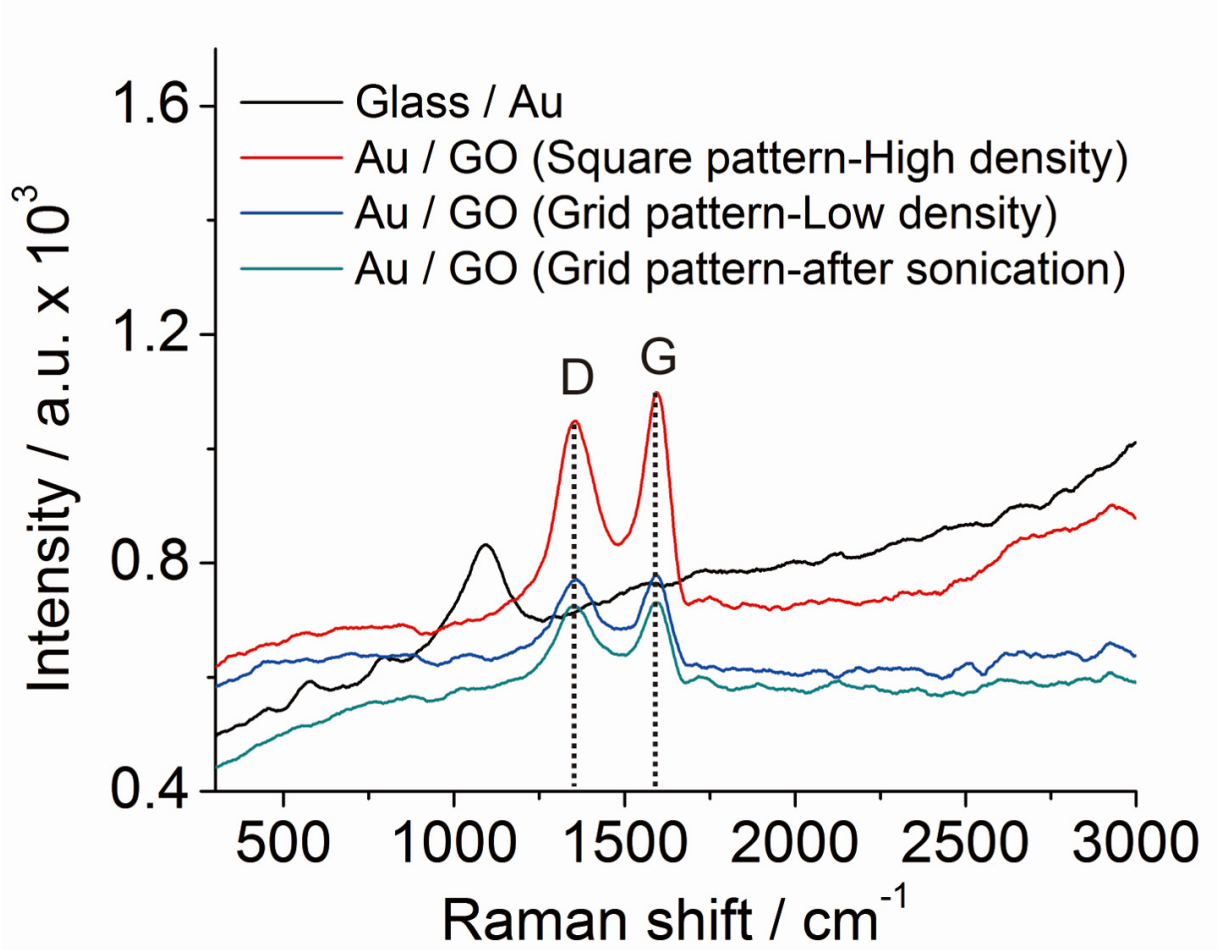

Supplementary Fig. 6 Raman spectra obtained from normal gold-coated glass substrate, NGO square pattern (5-50μm) on gold substrate, NGO grid pattern (10μm of line width with 200μm of spacing) on gold substrate and same NGO grid pattern after severe washing (ultrasonic cleaning with acetone, DIW and ethanol for 5 minutes each).

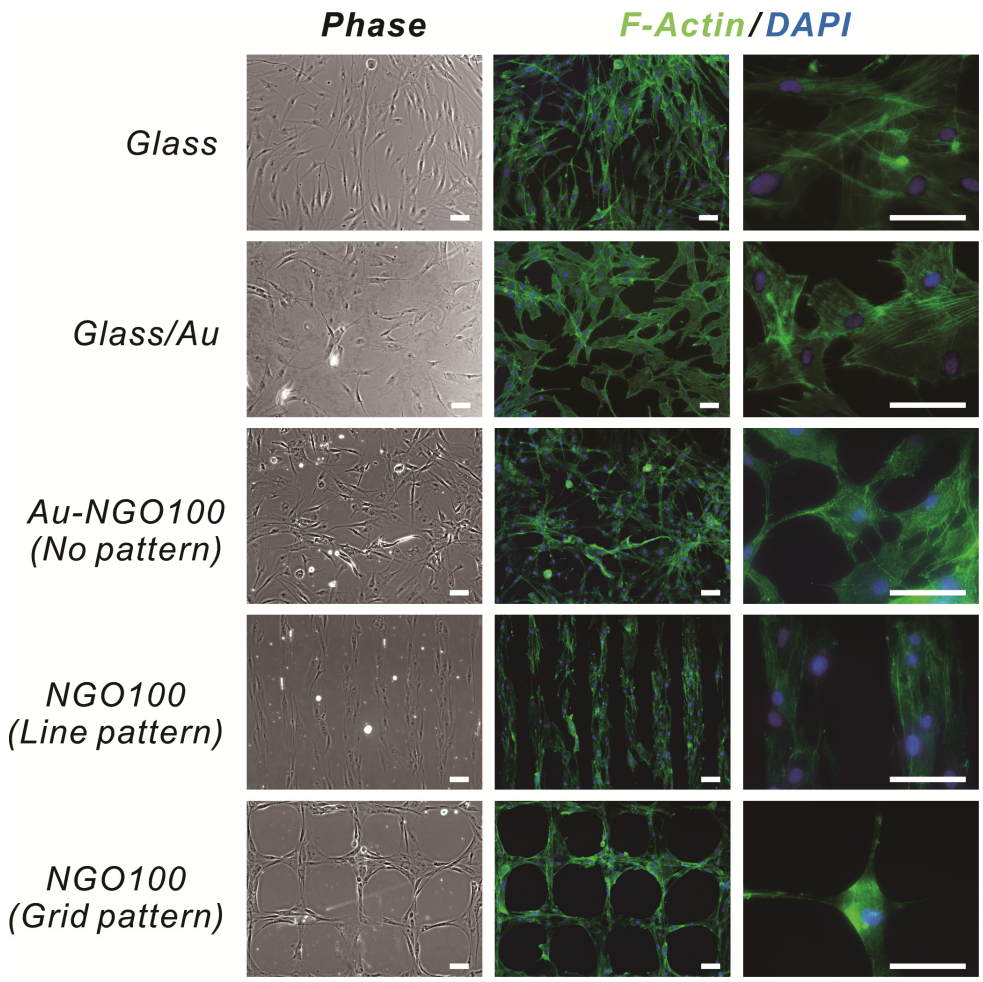

Supplementary Fig. 7 (a) Phase contrast and fluorescence images of hADMSCs stained for F-actin (green) and nucleus (blue) after two days of cultivation on different types of substrates including glass, gold-coated glass, NGO-coated gold, substrate with NGO line pattern and the substrate with NGO grid pattern. Scale bar = 50μm.

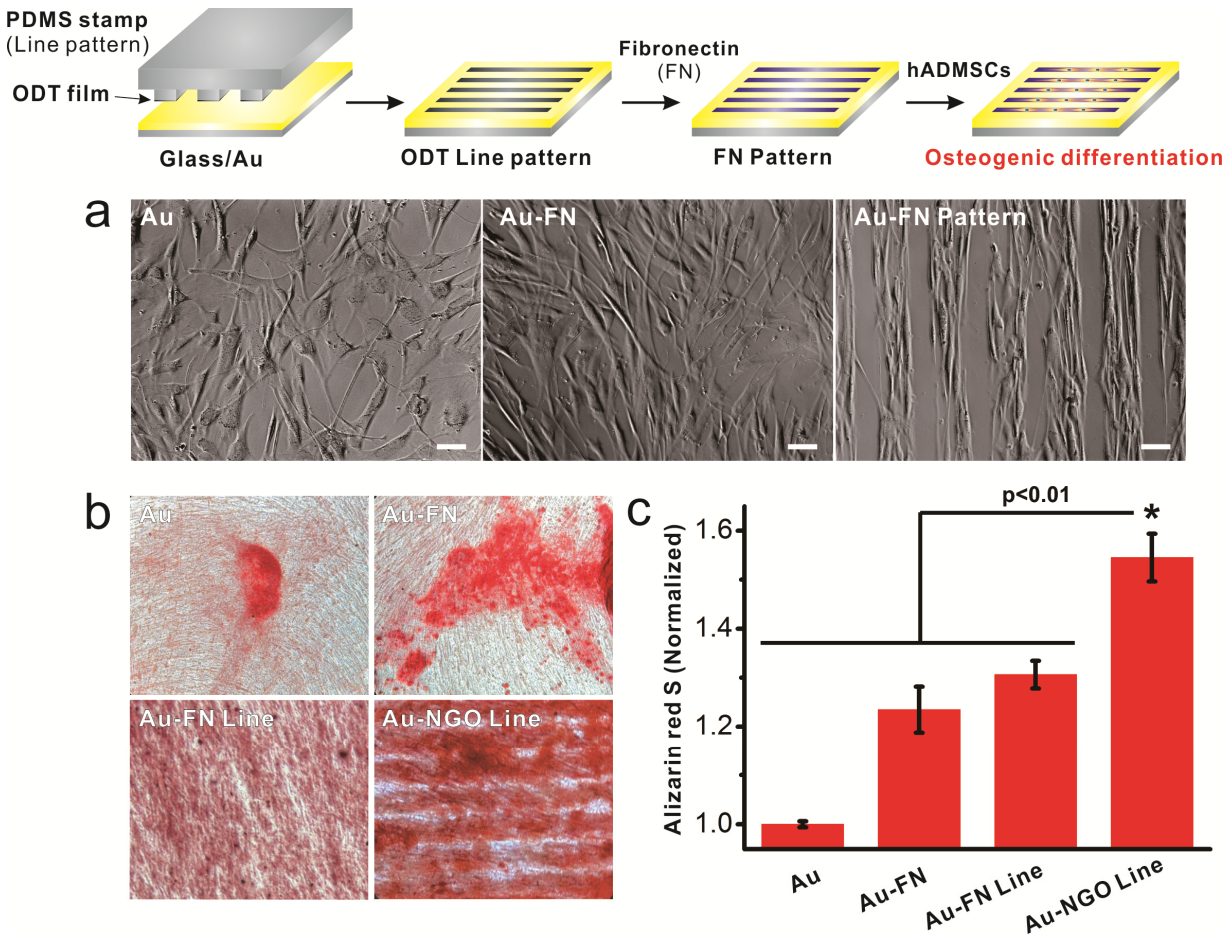

Supplementary Fig. 8 Comparison of hADMSC osteogenesis on different substrates. (a) Phase contrast images of hADMSCs on Au, FN-coated Au and FN-patterned Au. Scale bars = 20 μm. (b) Alizarin red S-stained images of hADMSCs differentiated into bone cells grown on four different substrates (Au, FN-coated Au, FN-patterned Au, NGO-patterned Au). (c) Quantitative comparison of calcification of cells grown on different substrates by extracting Alizarin red S used for staining calcium, normalized to control Au (n = 3; *p<0.01, Student's unpaired t-test).

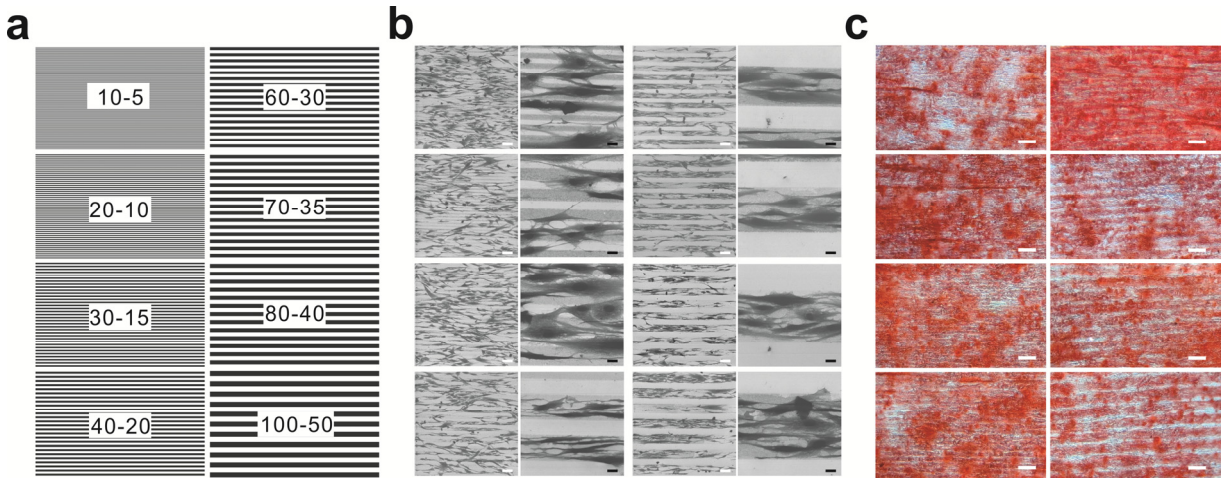

Supplementary Fig. 9 Effects of size of NGO line patterns on the calcification level of osteoblasts. (a) Size (first number) and the line separation (second number) of PDMS stamp used for the generation of NGO line patterns. (b) HIM images of hADMSCs following different sizes of NGO line patterns with different gap distances same as (a). Scale bar = 20μm (black) and 100μm (white). (c) Images showing the level of calcification of differentiated osteoblasts on NGO line patterns with different sizes and separations. Size and the gap distance between each line are same as (a). Scale bar = 100μm.

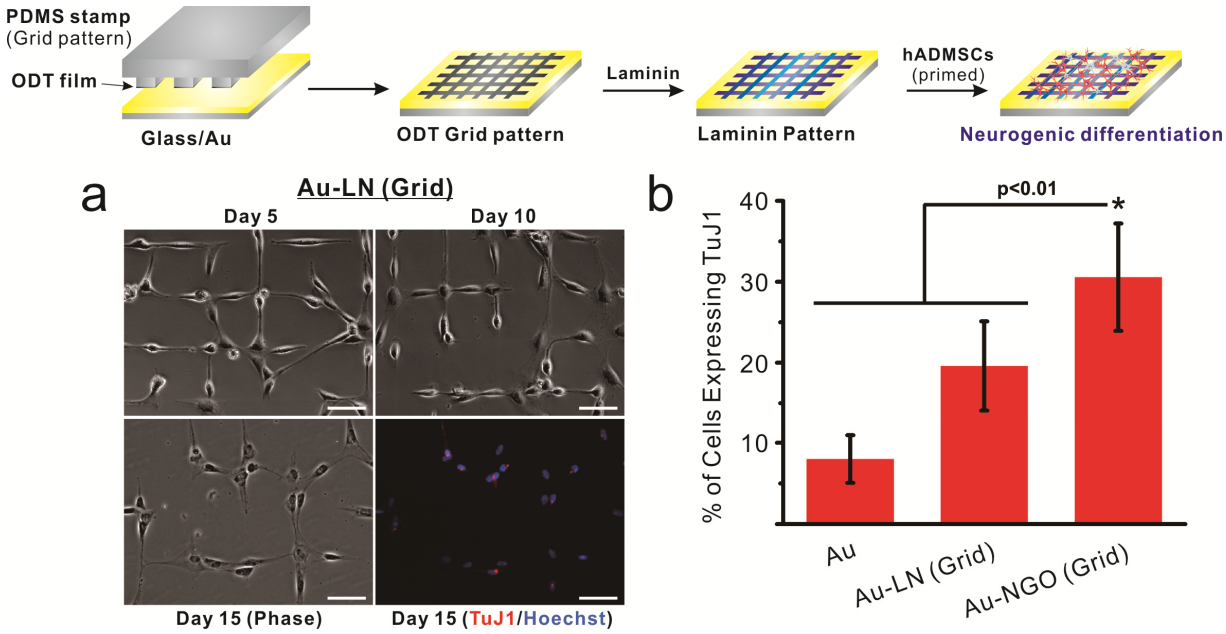

Supplementary Fig. 10 Neuronal differentiation of hADMSCs on laminin (LN)-coated substrates. (a) Phase contrast and fluorescence images of hADMSCs grown LN-patterned Au. Fluorescence images show staining for the neuronal marker TuJ1 (red) and nucleus (blue). Scale bars = 20 μm. (b) Quantitative comparison of the percentage of cell expressing the neuronal marker TuJ1 on PLL-coated Au [Au], LN-patterned Au [Au-LN (Grid)] and NGO grid-patterned substrates [Au-NGO (Grid)] (n = 3; *p<0.01, Student's unpaired t-test). All substrates were coated with LN to facilitate cell attachment.